

# The Mechanical Performance of a Novel Self-Adhesive Restorative Material

Ulrich Lohbauer<sup>a</sup> / Renan Belli<sup>b</sup>

**Purpose:** The development of a novel material requires a comprehensive pre-clinical assessment of clinical longevity before any market release. This study aimed to investigate the mechanical performance of a novel self-adhesive restorative material (ASAR MP4).

**Materials and Methods:** Fracture strength (FS), flexural fatigue strength (FFS) and fracture toughness ( $K_{Ic}$ ) were measured for the experimental material ASAR MP4 in self-cure (SC) and light-cure (LC) mode. ASAR MP4 was processed in capsules. Three direct resin composites (CeramX mono+, DentsplySirona; Heliomolar, IvoclarVivadent; Filtek Supreme XTE, 3M) and two glass-ionomer-cement (GIC) based materials (Equia Forte, GC; Fuji II LC, GC) were selected for comparison with ASAR MP4. FS specimens ( $n = 15$ ) were tested in a 4-point bending configuration according to ISO 4049 and 9917. FFS specimens ( $n = 25$ ) were additionally stressed for  $10^4$  loading cycles using the staircase approach. The single-edge-notch beam (SENB) configuration was selected for determining  $K_{Ic}$  according to ISO 13586. All specimens were stored for 14 days at 37°C. Data were analyzed using Weibull statistics (FS), ANOVA (FS,  $K_{Ic}$ ), and the non-parametric Mann-Whitney U-test (FFS).

**Results:** The FS, FFS and  $K_{Ic}$  data of the ASAR MP4 material reveal a mechanical performance in the range of the successful permanent direct resin composites CeramX mono+ and Heliomolar. The results for ASAR MP4 in SC mode were superior to the LC mode. A fine-grained and pore-free microstructure was observed.

**Conclusion:** Within the limitations of this study we conclude that the novel self-adhesive restorative material ASAR MP4 exhibits mechanical performance close to that of the resin composites Heliomolar and CeramX mono+, both indicated for permanent use in the load-bearing posterior region. Processing the material in either self-cure or light-cure mode led to superior performance over glass-ionomer cements.

**Keywords:** flexural strength, cyclic fatigue, fracture toughness, self-adhesion, resin composite, glass-ionomer cement.

*J Adhes Dent 2020; 22: 47–58.  
doi: 10.3290/j.ad.a43997*

*Submitted for publication: 15.09.19; accepted for publication: 16.01.20*

Due to the continuing discussions on the clinical use of dental amalgam, the Minamata convention of 2013 agreed on binding regulations for the phase down of mercury by 2020.<sup>39</sup> According to Regulation (EU) 2017/852 of the European Parliament and the European Council, each member state was requested to set out a national plan by 1 July 2019 to phase down the use of dental amalgam. By

30 June 2020, the Commission shall report to the European Parliament and the European Council on the outcome of its assessment regarding the feasibility of a phase out of the use of dental amalgam in the long term, preferably by 2030. This is a central concern for restorative dentistry, and has led to strong efforts to develop a substitute material for amalgam. The success of dental silver amalgam has multiple reasons, such as its ease of use as a direct packable material, its well-documented clinical longevity, and its cariostatic properties.<sup>30</sup> But most importantly, it presents an affordable alternative that meets the needs of a broad patient clientele, especially in poor and developing nations.

Since then, the dental industry has been eager to develop an alternative material to amalgam. Further to preventing caries, the dental community is outspoken on the need to guide efforts toward the development of general-purpose restorative materials.<sup>2</sup> In this context, simplified materials with self-adhesive properties have been identified as a major future trend.<sup>32</sup> Notwithstanding the comparable mechanical and clinical performance offered by other direct adhesively

<sup>a</sup> Associate Professor, Department of Restorative Dentistry and Periodontics, Research Laboratory for Dental Biomaterials, Friedrich Alexander University Erlangen-Nürnberg (FAU), Erlangen, Germany. Performed experiments, statistical analysis, wrote, revised and updated the manuscript.

<sup>b</sup> Research Associate, Department of Restorative Dentistry and Periodontics, Research Laboratory for Dental Biomaterials, Friedrich Alexander University Erlangen-Nürnberg (FAU), Erlangen, Germany. Performed experiments, proof-read and revised the manuscript.

**Correspondence:** Prof. Dr. Ulrich Lohbauer, Research Laboratory for Dental Biomaterials, Dental Clinic 1 – Operative Dentistry and Periodontology, Friedrich-Alexander University Erlangen-Nürnberg (FAU), Glueckstrasse 11, 91054 Erlangen, Germany. Tel: +49-9131-854-3740; e-mail: ulrich.lohbauer@fau.de

**Table 1** Materials, composition, and processing variables under investigation

Material	Manufacturer	LOT	Shade	Material class	Composition*	Processing
Equia Forte	GC	170807A	A2	GIC	PCA, aluminosilicate glass (70-80%, d <sub>50</sub> = 5 µm), water	Capmix (10 s), self-cure
Fuji II LC Capsule	GC	170713A	A2	RMGIC (LC)	PCA, HEMA, DMAEMA, CQ, aluminosilicate glass (70-80%, d <sub>50</sub> = 5 µm), water	Capmix (10 s), light cure (20 s)
ASAR MP4 SC	Dentsply Sirona	1807004175	A3	Self-adhesive restorative (SC)	Polycarboxylic acid, acrylic acid, bifunctional acrylate, water, self-cure initiator, CQ, glass fillers (d <sub>50</sub> = 2 µm), highly dispersed SiO <sub>2</sub> , YbF <sub>3</sub> , 77 wt% (58 vol%) fillers	Capmix (10 s), self-cure
ASAR MP4 LC	Dentsply Sirona	1807004175	A3	Self-adhesive restorative (LC)	PCA, AA, bifunctional acrylate, water, self-cure initiator, CQ, glass fillers (d <sub>50</sub> = 2 µm), highly dispersed SiO <sub>2</sub> , YbF <sub>3</sub> , 77 wt% (58 vol%) fillers	Capmix (10 s), light cure (20 s)
CeramX mono+	Dentsply Sirona	1706000833	M2	Resin composite	Dimethacrylate resins, CQ, methacrylate modified polysiloxane fillers (2-3 nm), SiO <sub>2</sub> nanofillers (10 nm), glass fillers (1 µm), 77wt% (55 vol%) fillers	Light cure (20 s)
Filtek Supreme XTE	3M Oral Care	N871882	A2	Resin composite	Bis-GMA, UDMA, TEG-DMA, PEG-DMA, bis-EMA, SiO <sub>2</sub> (20 nm) + ZrO <sub>2</sub> (4–11 nm) nanoclusters (0.6-20 µm), 78.5 wt% (63.3 vol%) fillers	Light cure (40 s)
Heliomolar	Ivoclar Vivadent	W34270	A2	Resin composite	Bis-GMA, UDMA, DDDMA, dispersed SiO <sub>2</sub> (<1 µm), YbF <sub>3</sub> , prepolymerized fillers	Light cure (20 s)

PCA: polycarboxylic acid; AA: acrylic acid; HEMA: hydroxyethylmethacrylate; DMAEMA: dimethylaminoethylmethacrylate; bis-GMA: bisphenol-A-glycidylmethacrylate; UDMA: urethandimethacrylate; TEG-DMA: triethyleneglycoldimethacrylate; PEG-DMA: polyethyleneglycoldimethacrylate; bis-EMA: ethoxylated bisphenol-A-dimethacrylate; DDDMA: decandioldimethacrylate; CQ: camphoroquinone. Manufacturer's information, scientific documentations, technical product files.

bonded materials such as resin composites,<sup>14, 23,34</sup> these suffer from drawbacks that include technique sensitivity and high cost, which limit their applicability on socioeconomic grounds. A recent editorial in this journal addressed the need for an amalgam-like material “combining the simplicity of glass-ionomer cements (GICs) with the stability of conventional composite without sacrificing the esthetic outcome”.<sup>41</sup>

The market offers GICs, hydrolytic acid-based cements with self-adhesion to tooth substrate that display cariostatic properties at interfaces.<sup>28,33</sup> The polyacidic matrix component, however, is not polymerizable, leading to a weak cohesive network and ultimately to low strength and wear resistance. GICs are indicated for provisional use up to extended class II cavities, thus not qualifying as complete replacement for amalgam in the permanent dentition. GICs are, however, a reliable alternative in pediatric dentistry due to the short lifetime of deciduous teeth.<sup>13</sup> Further processing in mixing capsules ensures a reproducible and safe application.<sup>28</sup>

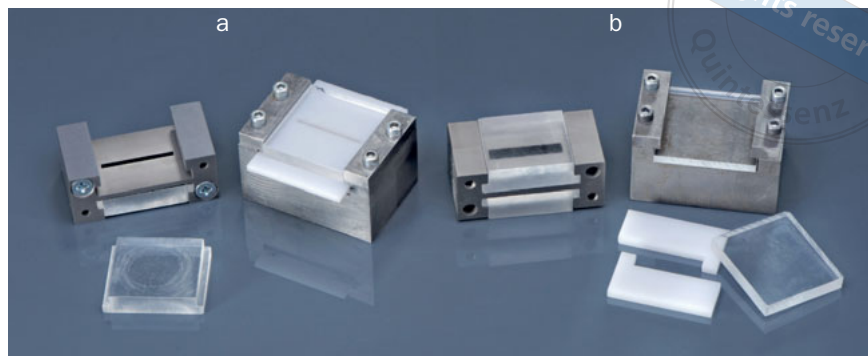
Resin-modified GICs (RMGICs) and compomers have been marketed as a hybrid material class combining the advantages of GICs and those of resin composites.<sup>24,33</sup> Polymerizable polyacid monomers provide the basis for the two-way setting reaction via an acid-base cement reaction combined with radical polymerization. Despite their long

market availability, these materials have failed to demonstrate sufficient mechanical stability to fulfill the criteria for permanent class II indication.<sup>13,22</sup>

Recently, the Dentsply Sirona (Konstanz, Germany) introduced a new concept of a self-adhesive resin-based material that promises amalgam-like properties and processing, with improved esthetic appearance compared to amalgam. This concept is termed ASAR (advanced self-adhesive restorative) and is on its way to being marketed under the name “Surefil one”.<sup>21</sup>

Although material development was not part of this study, the underlying chemical mechanisms need to be briefly introduced. The new concept focused on the development of a polymerizable acidic polymer enabling satisfactory adhesion that is still capable of achieving acceptable mechanical performance. Originating from research into compomer chemistry, the monomer development to date is summarized in a parallel article in this issue of the *Journal of Adhesive Dentistry*.<sup>21</sup> The key factor was to develop a monomer in which the content of carboxylic acid moieties remains high while supplying additional C=C double bonds to enable network polymerization. The central problem with this chemistry is the interaction between carboxylic acid and amino-based functional groups, necessary for radical

**Fig 1** Different molds to produce the specimens for FS (a), FFS (a), and  $K_{Ic}$  testing according to ISO 4049 and ISO 13586; a) tungsten-carbide molds for processing of resin composites, b) Delrin molds for processing GIC and ASAR MP4 materials.



polymerization. Finally, this research resulted in the development of a radically polymerizable amine functionalized protected monomer, called “MOPOS”.<sup>21</sup> However, the proof-of-concept of the polyacidic moieties in the resin network depends on the absorption of water in order to trigger the acid-base reaction. This might have major consequences on the network structure, as hydrolytic degradation, increased solubility, or dimensional expansion may occur.<sup>14,38</sup> Consequently, new diluent, hydrolytically stable monomers had to be synthesized and co-polymerized.

Hydrolytic effects are the most challenging concerns of dental materials as they are continuously exposed to an aqueous environment.<sup>29</sup> Long-term experiments have shown that the mechanical performance of resin composites decreases with water storage, while GICs improve over time due to a post-maturation effect.<sup>26</sup> However, it has been demonstrated in the past that “smart” ion-releasing materials which absorb water while releasing calcifying ions undergo considerable reduction in physical and mechanical properties upon water storage, leading to unsatisfactory clinical performance.<sup>6</sup> Water uptake also leads to hydraulic expansion in compomer materials, which are then able to fracture cemented crowns.<sup>38</sup> Similar effects have also been demonstrated for self-adhesive resin luting agents; the hydraulic pressure at the interface is very likely to exceed the hoop strength at crown margins that are already damaged by CAD/CAM machining.<sup>19</sup>

Another new approach claimed a bioactive component in a self-adhesive restorative formulation. This bioactive bulk-fill material initially showed promising mechanical performance similar to resin composites.<sup>1</sup> However, this concept failed clinically due to a high failure rate.<sup>40</sup> Discrepancies between experimental results and clinical survival might be due to the fact that laboratory experiments often disregard water-related phenomena.

The aim of the present study was to evaluate the mechanical performance of ASAR in the context of competitive GICs (acid-base, non-permanent in class II) and resin composites (polymerizable, permanent materials in class II). We investigated whether the ASAR material performs comparably to direct resin composites regarding quasi-static and fatigue properties after water storage.

## MATERIALS AND METHODS

### Materials

For comparison and classification of the novel and experimental direct restorative ASAR MP4 (advanced self-adhesive restorative), three conventional direct resin composites (CeramX mono+, Dentsply Sirona, Konstanz, Germany; Heliomolar, Ivoclar Vivadent, Schaan, Liechtenstein; Filtek Supreme XTE, 3M Oral Care, St Paul, MN, USA) and two glass-ionomer-type restorative materials (Fuji II LC and Equia Forte, GC; Tokyo, Japan) were selected. The ASAR MP4 material was employed in self-cure (SC) and light-cure (LC) modes. All materials are listed in Table 1. The resin composites were used in syringes while the GICs and the ASAR MP4 were used in capsules.

### Specimen Preparation for Flexural Strength (FS) and Flexural Fatigue Strength (FFS) Testing

As this project involved a variety of very different types of direct restorative materials, specimen preparation differed accordingly. The processing variables were selected for maximum intermaterial comparability.

The resin composites CeramX mono+, Heliomolar, and Filtek Supreme XTE were placed in a high-precision tungsten carbide mold (2 x 2 x 25 mm<sup>3</sup>) as shown in Fig 1a. Light polymerization was carried out with a halogen light curing unit (Elipar Trilight, 750 mW/cm<sup>2</sup>, 3M Oral Care) on five overlapping points on either the upper and lower side (in total 200/400 s light curing). All specimens for FS (n = 15) and FFS (n = 25) were produced in accordance with ISO 4049.<sup>18</sup> The irradiance of the curing unit was continuously monitored using an integrating sphere (Ulbricht-Kugel, Gigahertz Optik; Türkenfeld, Germany).

The glass-ionomer type materials Fuji II LC and Equia Forte, and the experimental ASAR MP4 materials were processed in accordance with ISO 4049 and ISO 9917. The materials were handled under calibrated conditions of 23°C and 50% relative humidity. All materials were delivered as capsule products and mixed in a standard mixing device (Capmix, 3M Oral Care) for 10 s. The materials were placed in a special Delrin mold (DuPont; Wilmington, DE, USA) (2 x 2 x 25 mm<sup>3</sup>, see Fig 1a) and condensed. One capsule

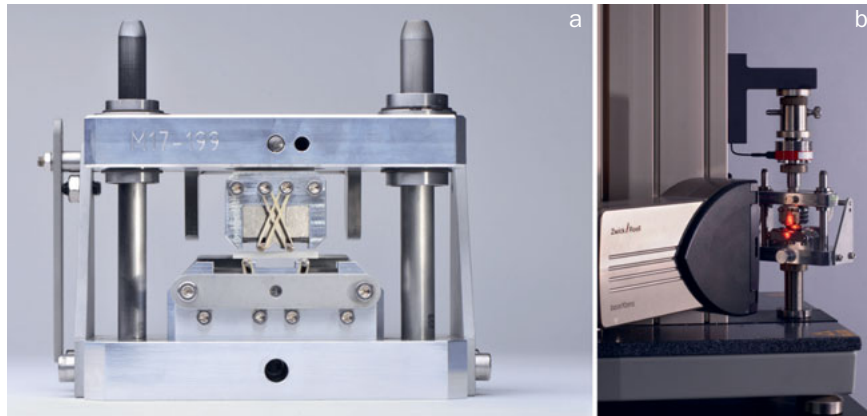


**Fig 2** The test setup used for four-point flexural strength testing, a) a custom made test rig adjustable to various roller configurations and span lengths, b) speckle image correlation for precise strain control.

matched the volume of one specimen. If required, light curing was performed in the same way as described for resin composites.

In order to ensure a proper maturation process, only the self-cure materials were stored in a water bath at 37°C for 10 min (still in the molds), thereby preventing dehydration and ion leaching in storage water. This step was mandatory in order to reach a proper maturation for further handling. Light curing, if required, was performed after placement in the mold. After removing from the mold, the materials were pre-stored in 100% relative (air) humidity for 1 h at 37°C. All materials were then stored for 14 days in distilled water at 37°C. Prior to testing, the specimen flanges were finished (removal of edge defects) with of 1200-grit SiC paper under continual water cooling. No coating was applied.

### Initial Fracture Strength (FS) and Flexural Fatigue Strength (FFS) Measurements

The FS ( $\sigma_f$ ) was evaluated using the 4-point bending setup (Fig 2a) in a universal testing machine (Zwick Z2.5, Zwick; Ulm, Germany).<sup>17</sup> The 100-N load cell was calibrated, and testing was performed at a crosshead speed of 0.75 mm/min. An external laser extensometer with laser beam illumination (laserXtens, Zwick) was used to track the true displacement on the specimen using the speckle image correlation method (Fig 2b). The test rig was set to 10/20 mm of the upper/lower support rollers in accordance with ISO 4049.

The initial fracture strength ( $\sigma_f$ ) was calculated using the equation:

$$\sigma_f = \frac{3PL}{4wb^2}$$

where P is the maximum load at failure, L the distance between the lower supports (20 mm), w the width (ca 2 mm, individually measured) and b the height of the specimen (ca 2 mm, individually measured).

As the materials under investigation are assumed to fracture in a brittle manner, Weibull statistical analysis was used.<sup>35,36</sup> The Weibull approach describes the failure probability  $P_F$  as

$$P_F = 1 - \exp \left[ - \left( \frac{\sigma_f}{\sigma_0} \right)^m \right]$$

in which the Weibull shape parameter  $m$  and characteristic scale parameter  $\sigma_0$  were determined in a double-logarithmic plot of

$$\ln \ln \frac{1}{1 - P_F} = m \ln \sigma_f - m \ln \sigma_0$$

The slope of the regression describes the scatter in strength and gives the  $m$  value, while  $\sigma_0$  represents the strength at a failure probability of  $P_F = 63.2\%$  when  $\ln(\ln(1/(1 - P_F))) = 0$ . A more clinically relevant scale parameter,  $\sigma_{0,05}$ , can be obtained from the plot and represents the strength at a failure probability of  $P_F = 5\%$  when  $\ln(\ln(1/(1 - P_F))) = -2.97$ .

The flexural fatigue strengths (FFS) of the materials examined were determined for  $10^4$  loading cycles under equivalent test conditions at a frequency of 0.5 Hz. The “staircase” method was used for the fatigue resistance evaluation.<sup>5,8,9,25</sup> For each cycle, the stress amplitude alternated between 1 MPa and maximum stress. Tests were conducted sequentially, with the maximum applied stress in each succeeding specimen being increased or decreased by a fixed increment of stress, according to whether the previous  $10^4$  cycle run resulted in failure or survival. The first specimen was tested at 50% of the initial mean fracture strength value. All tests were carried out in water at 37°C. FFS and standard deviation (SD) were determined using equations 2 and 3, respectively.<sup>8,9</sup>

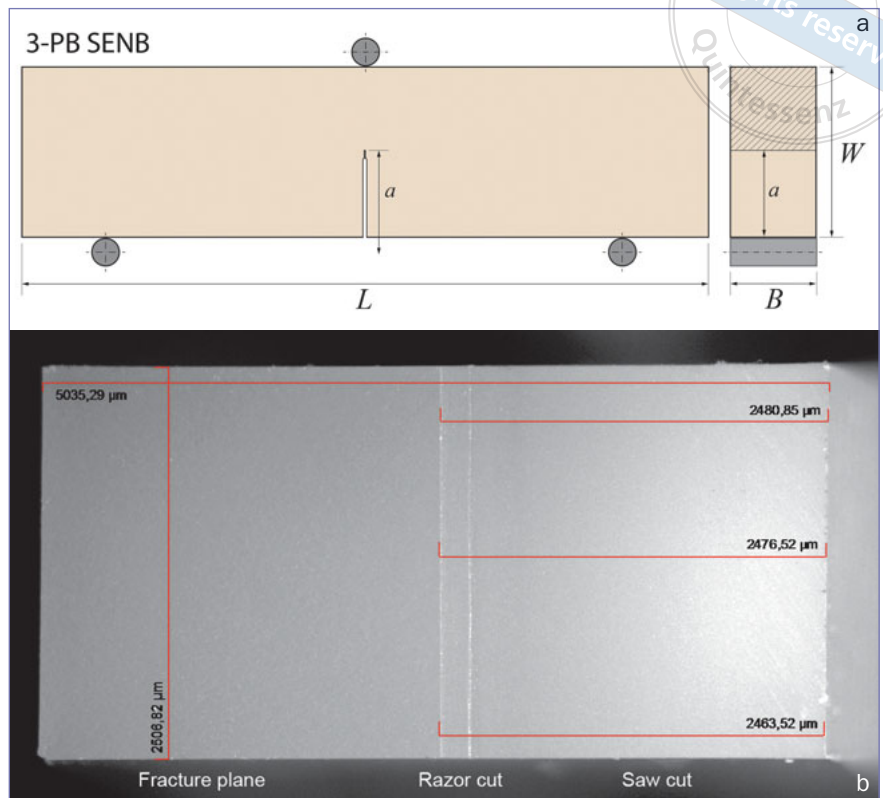
$$FFS = X_0 + d \left( \frac{\sum \ln i}{\sum n_i} \pm 0.5 \right)$$

$$SD = 1.62d \left( \frac{\sum n_i \sum i^2 n_i - (\sum \ln i)^2}{(\sum n_i)^2} + 0.029 \right)$$

In Equation 4,  $X_0$  is the lowest stress level considered in the analysis and  $d$  is the fixed stress increment. To determine FFS, the analysis of the data is based on the least



**Fig 3** Schematic specimen configuration for SENB testing according to ISO 13586 (a). Measurement of the notch depth from a fractured specimen under the light microscope (b).



frequent event (failures versus survivals). The negative sign is used when the analysis is based on failures, otherwise the positive sign is used. In Equations 4 and 5, the lowest stress level considered is designated  $i = 0$ , the next  $i = 1$ , and so on, and  $n_i$  is the number of failures or survivals at the given stress level.

### Fracture Toughness ( $K_{Ic}$ ) Specimen Preparation and Measurement

Fracture toughness ( $K_{Ic}$ ; C = critical, unit:  $\text{MPam}^{0.5}$ ) was measured according to ISO 13586.<sup>18</sup> This standard is derived from the classic ASTM E399 standard for testing of the SENB (single-edge-notch beam) configuration, as shown in Fig 3.

Specimen bars of dimensions  $2.5 \times 5 \times 25 \text{ mm}^3$  ( $n = 15$  per material) were manufactured in a tungsten carbide mold of appropriate dimensions (see Fig 1b). The materials were selected according to Table 1 and processed as described above for FS and FFS specimens. The GIC and ASAR MP4 materials were processed in an analogous Delrin mold, as described above. Two capsules were used for production of one specimen. The material portions were placed in bulk so that the increment interface did not affect the central part of the notch. Storage conditions were applied as described above.

SENB specimens require a defined notch perpendicular to the long axis of the specimen (see Fig 3). To achieve this, notches in the center of the specimens were prepared orthogonal to their width ( $w$ ) plane. Through-the-thickness

notches were sawed using 0.2-mm-thick diamond disks and further sharpened (in length  $> 150 \mu\text{m}$ ) with razor blades and alumina paste ( $3\text{-}1 \mu\text{m}$ ) to reach a final notch length  $a$ , of  $a/w = 0.5$ , and notch tip root radius  $< 6 \mu\text{m}$ . The preparation of the notches was performed 24 h after specimen production, due to insufficient mechanical stability of the GIC specimens to notching, as the cutting procedure very likely induced premature fractures.

The measurements were conducted in a 3-point bending test. The test setup in Fig 2a was adjusted to one central upper roller. The measurements were conducted in the universal testing machine (Z2.5, Zwick) described above at  $10 \text{ mm/min}$ , an adaptation recommended by ISO 13586 to eliminate any visco-elastic effect and to ensure a pure linear-elastic material response.<sup>5,18</sup> After fracture, the crack length ( $a$ ) was measured at three points along the notch width using a stereomicroscope (STEMI V6, Zeiss, Germany), as shown in Fig 3. The fracture toughness was calculated using the equation:<sup>31</sup>

$$K_{Ic} = f\left(\frac{a}{w}\right) \frac{F}{h\sqrt{w}}$$

where  $F$  represents the load at fracture,  $a/w$  is the crack length ratio and  $f(a/w)$  is a geometry calibration factor depending on the crack length  $a$ , available in ISO 13586.<sup>18</sup>

**Table 2** Weibull parameters  $\sigma_0$ ,  $\sigma_{0.05}$ , and  $m$  with respective 90% confidence intervals, FS (mean values [SD]), FFS (SD) and FFS% (remaining strength after fatigue loading), as well as the fracture toughness ( $K_{Ic}$  [SD]) results for the materials under investigation

Material	$\sigma_0$ [MPa]	$\sigma_{0.05}$ [MPa]	$m$	$\sigma_f$ [MPa]	FFS [MPa]	FFS% [%]	$K_{Ic}$ [MPam <sup>0.5</sup> ]
Equia Forte	33.08 (29.43–37.28)	14.33	4.1 (2.7–5.3)	29.95 (8.87) <sup>a</sup>	16.83 (5.5) <sup>a</sup>	56.19	0.55 (0.03) <sup>b</sup>
Fuji II LC	57.20 (54.07–60.61)	43.47	8.9 (5.7–11.5)	54.24 (6.78) <sup>b,c</sup>	22.57 (1.84) <sup>b</sup>	41.61	0.89 (0.12) <sup>a</sup>
ASAR MP4 SC	51.76 (48.36–55.48)	33.85	6.6 (4.4–8.5)	48.43 (8.12) <sup>b</sup>	34.65 (1.91) <sup>e</sup>	71.54	0.79 (0.06) <sup>d,e</sup>
ASAR MP4 LC	60.91 (57.44–64.66)	43.33	8.2 (5.4–10.6)	57.61 (7.81) <sup>c,d</sup>	29.22 (3.41) <sup>d</sup>	50.72	0.72 (0.09) <sup>c</sup>
CeramX mono+	69.19 (64.45–74.40)	44.26	7.0 (4.5–9.2)	64.63 (11.31) <sup>d</sup>	25.22 (4.9) <sup>c</sup>	39.02	0.83 (0.03) <sup>e</sup>
Heliomolar	62.44 (59.97–65.08)	49.45	12.4 (7.9–16.1)	59.96 (5.52) <sup>c,d</sup>	33.03 (1.23) <sup>e</sup>	55.09	0.74 (0.04) <sup>c,d</sup>
Filtek Supreme XTE	114.78 (106.74–123.63)	73.95	6.6 (4.3–8.6)	107.18 (18.64) <sup>e</sup>	51.93 (6.76) <sup>f</sup>	48.45	1.03 (0.08) <sup>f</sup>

Superscript letters indicate statistically homogeneous subsets within each variable.

### Statistical Analysis

The applicability of FS data distribution regarding a Gaussian or Weibull distribution was tested using the Kolmogorov-Smirnov or the modified Kolmogorov-Smirnov D test, respectively. As FS data could not be determined regarding either a Gaussian or a Weibull distribution, Weibull statistics were selected to show the characteristic strength in terms of failure probability.<sup>7</sup> In order to report unbiased estimations for the Weibull  $\sigma_0$  and  $m$  data, specific weighting factors were used regarding the number of tested specimens ( $n = 15$ ).<sup>7,18</sup> Mean FS and  $K_{Ic}$  data were further analyzed using the one-way ANOVA test and S-N-K post-hoc test using a critical value of 95% significance ( $\alpha = 0.05$ ). As the FFS analysis is based on the various stress levels  $X_i$ , the non-parametric Mann-Whitney U-test was applied. Calculations were performed using the IBM SPSS 21 software package (IBM; Armonk, NY, USA).

## RESULTS

### Fracture Strength and Flexural Fatigue Strength

Table 2 summarizes all mechanical data calculated from FS, FFS, and  $K_{Ic}$  experiments after 14 days of water storage at 37°C. Among all materials, Filtek Supreme XTE showed a significantly positive effect in terms of the statistically highest values regarding FS, FFS, and  $K_{Ic}$ . The GIC Equia Forte, at the other extreme, exhibited a significantly negative effect and the statistically weakest FS, FFS and  $K_{Ic}$  data. In general, the GIC materials ranked lowest, while the resin composites exhibited superior behavior. The results from the novel material, ASAR MP4, fell between those of GIC

and resin composites. For all three measurements, both ASAR MP4 versions achieved results in the range of the resin composite, Heliomolar.

Figure 4 shows the Weibull plots for all FS data. A Weibull characteristic strength of  $\sigma_0 = 60.91$  MPa and a Weibull modulus of  $m = 8.2$  was calculated for the material ASAR MP4 LC. Assuming a 5% failure rate, the characteristic strength will only hold for  $\sigma_{0.05} = 43.33$  MPa. The statistically highest characteristic strength of  $\sigma_0 = 114.78$  MPa was found for Filtek Supreme XTE and the least scatter of data was found for Heliomolar, expressed by a Weibull modulus of  $m = 12.4$ . Comparing both materials, Filtek Supreme XTE showed a FS almost twice that of Heliomolar. However, taking the scatter of data into account and considering the more clinically related analysis at a failure probability of only 5%, Heliomolar shows a strength level of  $\sigma_{0.05} = 49.45$  MPa, compared to Filtek Supreme XTE with  $\sigma_{0.05} = 73.95$  MPa, a value only 1.5 times greater than that of Heliomolar. Figure 5 exhibits all data points and respective profiles regarding the staircase fatigue tests. In terms of remaining FFS% after fatigue loading, the ASAR MP4 SC performed best, showing only a 28.5% drop from initial FS. Figure 6 shows all data points regarding the fracture toughness tests with a significantly positive effect for  $K_{Ic}$  of Filtek Supreme XTE and a significantly negative effect for the RMGIC material Fuji II LC. In Fig 7, a comparison between FS vs FFS data is drawn, as the material response under quasi-static loading should produce an outcome different than would cyclic fatigue loading.<sup>18,25</sup>

Materials above the dotted line (such as ASAR MP4 SC or Heliomolar) are those with a greater fatigue resistance ratio compared to materials below the dotted line (Fuji II LC or CeramX mono+). The line simply indicates a drop in

**Fig 4** Weibull plots for all materials under investigation showing the characteristic strengths  $\sigma_0$  for a failure probability of  $P_F = 63.2\%$  and  $\sigma_{0.05}$  for a failure probability of  $P_F = 5\%$ .

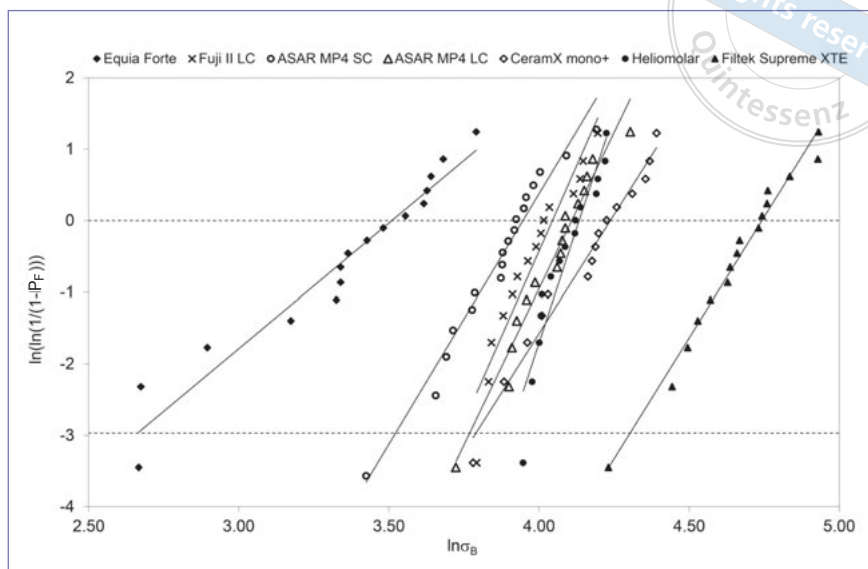
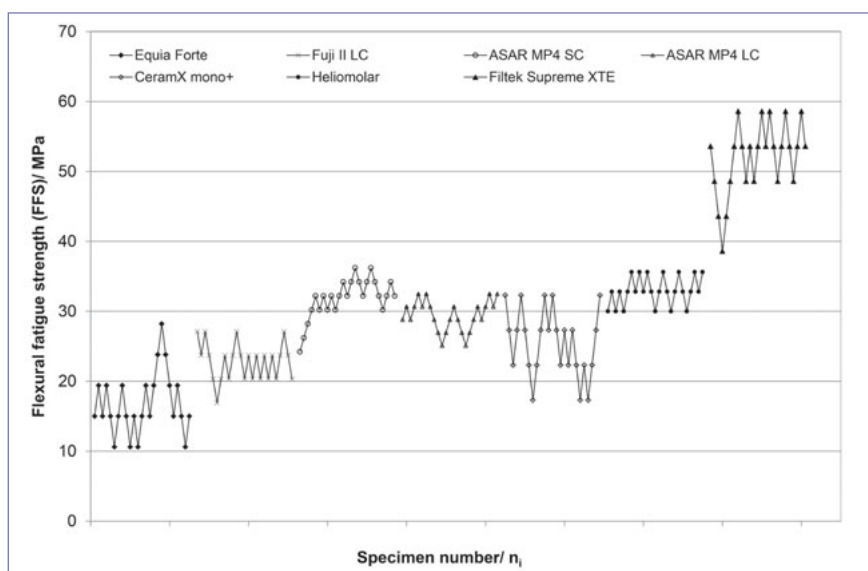


**Fig 5** FFS data for all materials under investigation showing their respective “staircase” profiles.



strength of 50% which is matched by the materials Equia Forte, ASAR MP4 LC, and Filtek Supreme XTE.

## DISCUSSION

FS data, measured strictly according to an ISO standard (eg, ISO 4049 or ISO 9917) present values of limited validity. ISO standards have established minimum common ground regarding testing procedures and complexity. Standards serve as a screening tool characterizing and ranking materials on a worldwide basis. For specific applications such as in dentistry, at least storage conditions and loading scenarios need to be added in order to obtain a clinically relevant picture of a material.<sup>5</sup> For example, ISO 4049 re-

quires 24 h storage in 37°C water, although it is a well-known fact that hydrolytic degradation is a continuous process over of a much longer period of time.<sup>11,26</sup> Our results show FS data after 14 days water storage at 37°C, probably already reduced compared to strict ISO testing (24 h) or even to dry conditions.<sup>20</sup> By simulation of the mastication process over time, we selected cyclic loading over 10,000 cycles, represented by the FFS data under investigation (Table 2). All materials further degrade under mechanical loading, showing a strength reduction from FS to FFS between 28.5% (ASAR MP4 SC) and 61% (CeramX mono+).

Ultimately, FFS data might be considered the more clinically relevant predictor. In a recent guidance on resin composite testing, the lack of correlation between FS and clinical studies was discussed.<sup>17</sup> Although restoration fracture

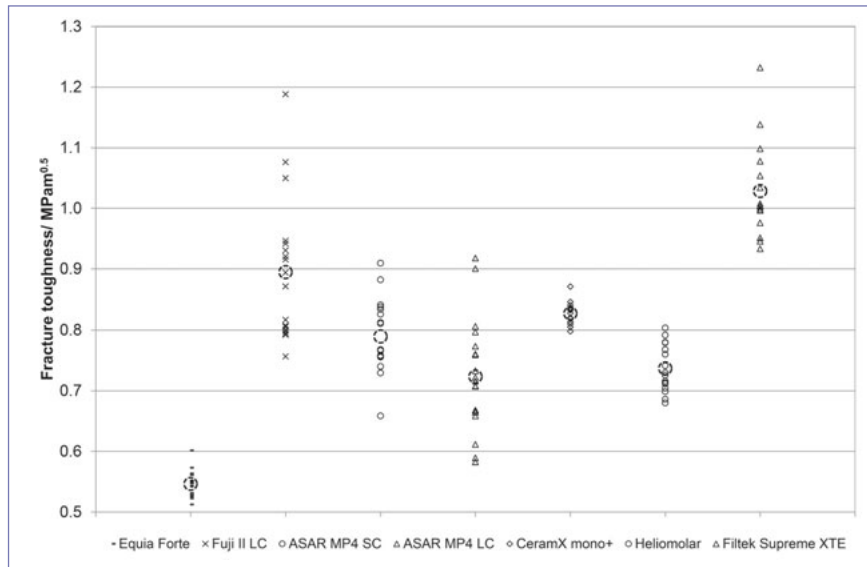


**Fig 6**  $K_{Ic}$  data for all materials under investigation including the mean value (bold circles).

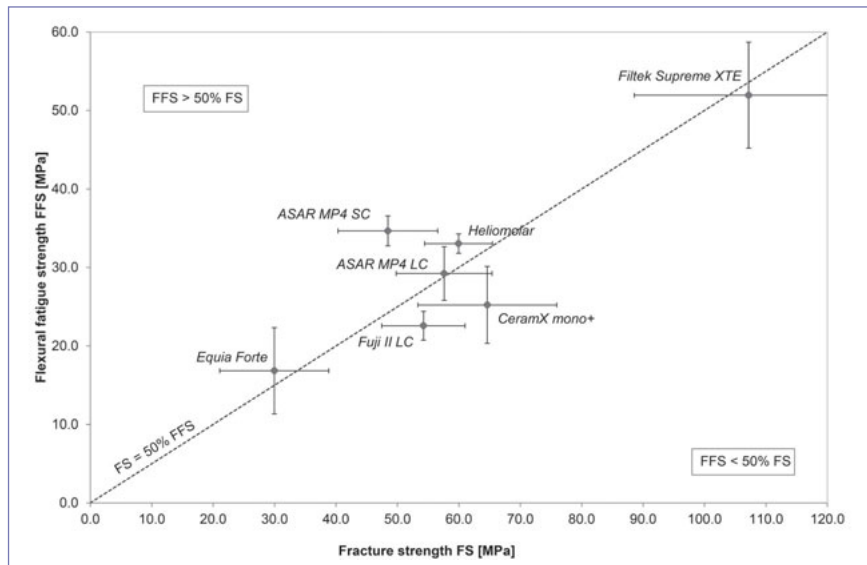


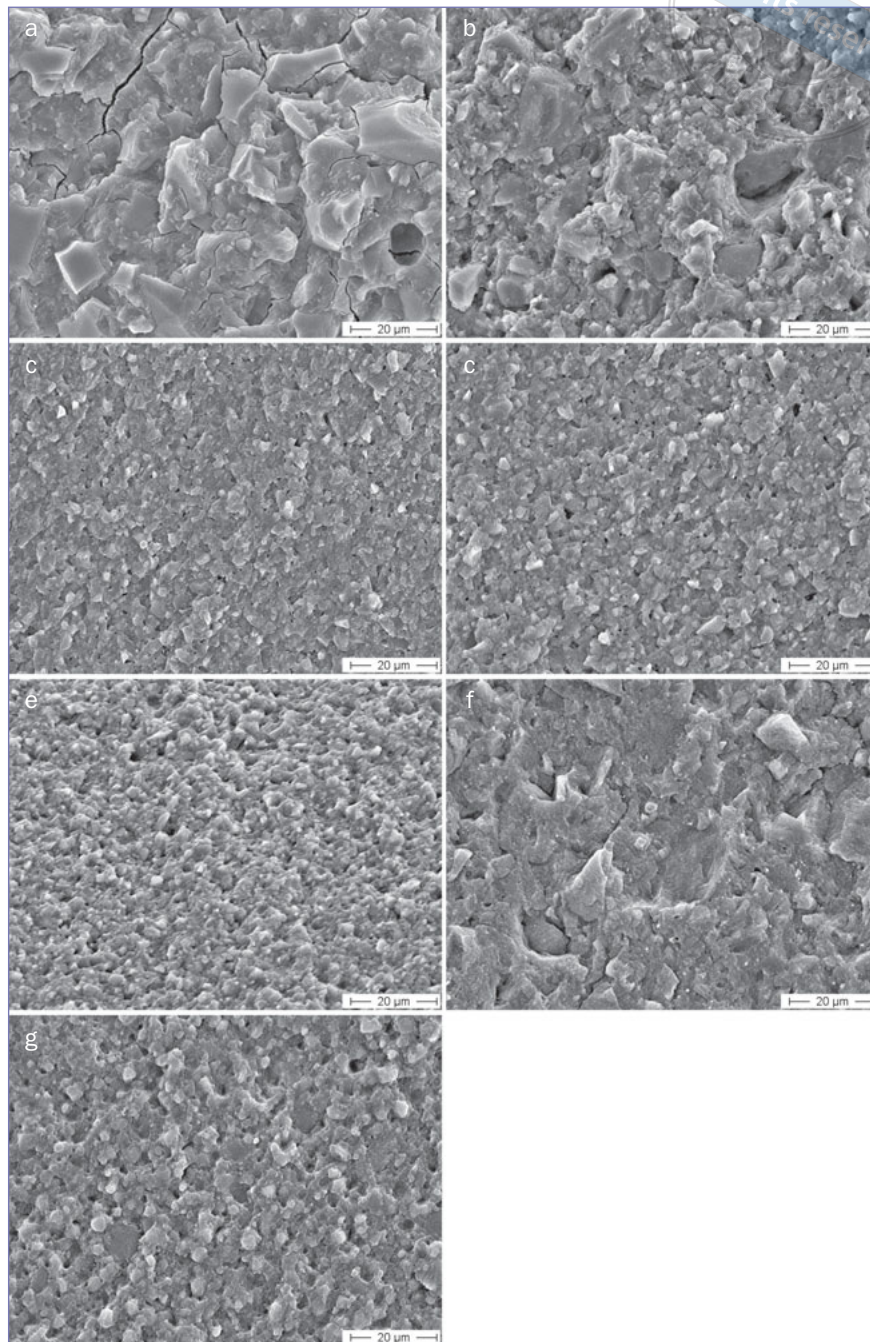
**Fig 7** FS vs FFS plot with standard deviations indicating their strength loss. Materials below the dotted 50% FS line exhibit a weaker remaining FFS compared the 50% FS drop. Materials above this line show a greater remaining FFS compared to a 50% drop in FS.

has been found to be one of the most prevalent causes of clinical failure, only a weak correlation with fracture strength data from posterior composites could be established.<sup>16</sup> As extensive clinical evidence is expensive and time consuming, the research community is investigating certain material properties and testing procedures that are able to reflect and predict clinical reality already in the pre-clinical development phase. Among other factors, the mechanical performance of materials has been termed one of the most critical parameters for a material's clinical indication and longevity.<sup>10,12</sup> Although the authors have found no clear correlation between laboratory testing and clinical performance, wear, toughness, and fatigue resistance were addressed as expected and suitable clinical predictors, especially for materials showing ceramic-like brittle behavior.<sup>42</sup>

The mechanical evaluation shown here presents further data for fracture toughness and fatigue resistance. FFS testing revealed the highest fatigue resistance for resin composites (Filtek Supreme XTE: FFS = 51.93 MPa) and the lowest for GIC (Equia Forte: FFS = 16.8 MPa). This finding is generally correlates with clinical indications: Resin composites are materials indicated as permanent restoratives in the load-bearing molar region, while GICs are still considered as provisional (or semi-definitive) materials for the permanent dentition. In class II, GICs are today indicated only in small cavities with no involvement of the marginal ridge.<sup>19</sup> The correlation between FFS and clinical outcome has also been shown for other direct and indirect materials.<sup>14,15,27</sup> The material development of ASAR MP4 showed slightly better results for the self-curing (FFS = 34.6 MPa) than the light-



**Fig 8** SEM microstructural images of the fracture planes. Equia Forte (a) and Fuji II LC (b) show disintegrated particles and residual porosity. Particle sizes of both GIC are between 10-20  $\mu\text{m}$ . Microcracks are observable due to dehydration in the high vacuum SEM mode. The materials ASAR MP4 SC (c) and ASAR MP4 LC (d) show similar and fine grained microstructure with particles below 5  $\mu\text{m}$  ( $d_{50} = 2 \mu\text{m}$ ). Microporosity (voids below 1  $\mu\text{m}$ ) are observable in both materials. The resin nanohybride composite material CeramX mono+ (e) exhibits a homogeneous microstructure with particle sizes of approximately 3  $\mu\text{m}$ . Heliomolar (f), the inhomogeneous microfiller composite, shows large prepolymerized fillers of up to 20  $\mu\text{m}$  diameter. Filtek Supreme XTE (g) as a nanohybride composite shows a similar microstructure to CeramX mono+ with fillers of around 3  $\mu\text{m}$  diameter.



curing (FFS = 29.2 MPa) version, performing statistically similar to Heliomolar (FFS = 33.0 MPa) and better than CeramX mono+ (FFS = 25.2 MPa). Figure 7 shows that the FS:FFS ratio is superior for ASAR MP4 SC compared to other GIC and even resin composites, as the remaining FFS only drops to a level of 71.5% of the initial FS. The higher initial FS of ASAR MP4 in LC mode is a consequence of the nature and size of surface and subsurface defects controlling fracture. As FFS is highly related to bulk properties and  $K_{Ic}$  is measured on one single artificial crack in the bulk of the

specimen, the higher FFS and  $K_{Ic}$  of the SC version suggests a more dense and homogeneous structure in the bulk of the matrix.<sup>18,25</sup>

Fracture toughness is a property that describes the ability of a material containing a crack to resist fracture, and is one of the most important properties of any material for virtually all design applications. Inherent surface defects (eg, surface scratches) are able to grow under mechanical stress until they reach a critical size, leading to material failure. A material with a high fracture toughness is able to

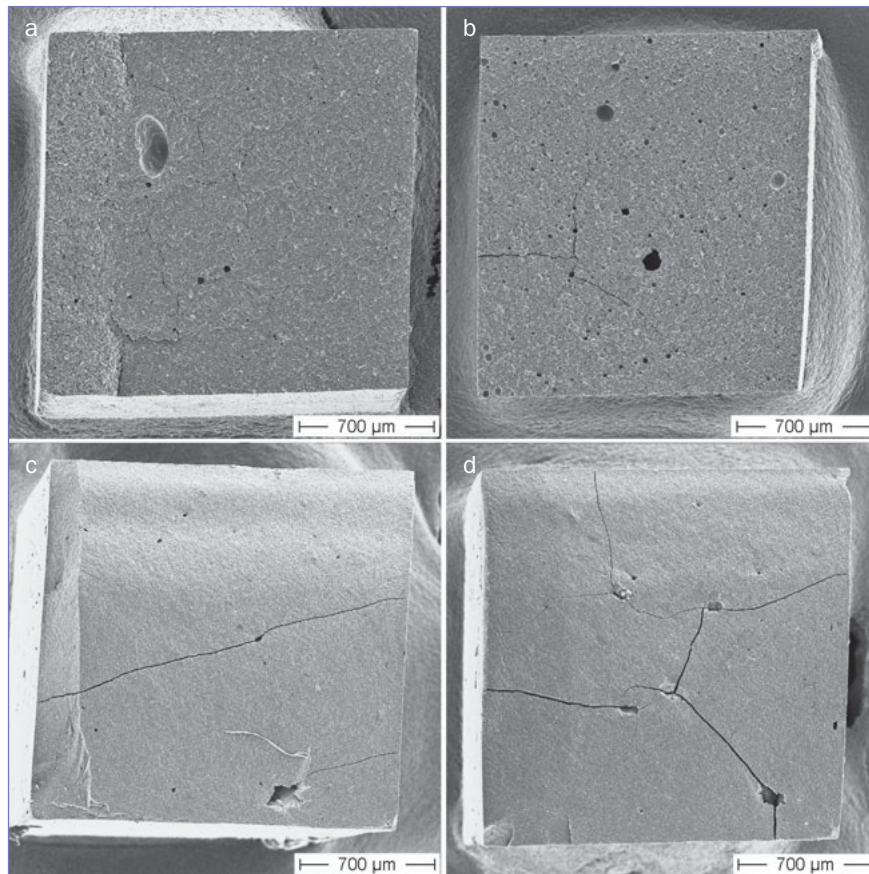


**Fig 9** SEM analysis from fractured FS test specimens of the capsule mixed products showing considerable residual porosity (< 10%) for both GIC Equia Forte (a) and Fuji II LC (b). The materials ASAR MP4 SC (c) and the LC version (d) show a smooth and homogeneous surface with no major sign of porosity. Crack formation on the materials' surface is due to dehydration in the high vacuum SEM.

better resist the crack growth. In consequence, under high loading situations, materials with a high  $K_{Ic}$  are less sensitive to surface defects and more reliable (damage tolerant). The fracture toughness data measured according to ISO 13586 showed the statistically highest value of  $K_{Ic} = 1.03$  MPam<sup>0.5</sup> for the material Filtek Supreme XTE. Regarding the experimental formulation ASAR MP4, the self-cure version led to a significantly positive effect in fracture toughness ( $K_{Ic} = 0.79$  MPam<sup>0.5</sup>) compared to the light-cure counterpart ( $K_{Ic} = 0.72$  MPam<sup>0.5</sup>), both being in the range of Heliomolar ( $K_{Ic} = 0.74$  MPam<sup>0.5</sup>) and slightly below the CeramX mono+ values ( $K_{Ic} = 0.83$  MPam<sup>0.5</sup>). In a recent study, the present authors compared several resin-based composites with respect to a comparison of linear-elastic material properties such as elastic modulus, fracture strength, and fracture toughness with cyclic fatigue resistance, as measured here.<sup>3</sup> Based on 12 different resin composite materials, we were unable to establish a reliable correlation between fracture toughness and FFS,<sup>3</sup> concluding that the clinical relevance of fracture toughness is limited, if only considered in the linear-elastic range related to crack size  $a$ . In terms of strain energy release rate ( $G_{Ic} = K_{Ic}^2/E/(1-\nu^2)$ ), the mechanical energy consumed for the fracture event in resin composites is higher than that of many ceramics, due to the inverse relationship to the Young's modulus  $E$  ( $\nu$  is the

Poisson ratio).<sup>4</sup> The decrease in  $E$  due to water hydrolysing and plasticising effects is expected to increase the energy consumed in water-stored resin composites, but this effect is neglected if only  $K_{Ic}$  is measured. ISO 13586 describes a solution for treating visco-elastic materials with the energy criterion.<sup>18</sup> For certain individual restoration designs, such as thin margins, sharp edges, cusps, or prominent marginal ridges, the chipping susceptibility of restorative materials plays a major role. The chipping resistance is preclinically assessed by measuring the toughness, eg, edge toughness.<sup>37</sup>

The microstructure of the materials under investigation is shown in Fig 8. The images were taken from fractured FS specimens. Different microstructural features such as filler sizes and porosity can be seen. One of the most prominent differences is the coarse microstructure of GIC compared to the fine, smooth appearance of both ASAR MP4 SC and LC modes ( $d_{50} = 2 \mu\text{m}$ ). Figures 8c and 8d seem to highlight either some microporosity from the mixing procedure or microvoids from disintegrated filler particles. A further conclusion is not possible, as further analysis is required. Within the resin composites, Heliomolar shows a comparably coarse microstructure with particles up to 20  $\mu\text{m}$  in diameter, reflecting the pre-polymerized filler technology used in this material. The nanohybrid materials CeramX mono+



and Filtek Supreme XTE show a fine microstructure with nanospheres or nanoclusters in the range below 3  $\mu\text{m}$ .

Figure 9 shows an overview of the capsule mixed products. The images were taken from fractured FS specimens. Figures 9a and 9b show obvious porosity (> 10%), while ASAR MP4 exhibited reduced porosity, commonly entrapped during capsule mixing. This might be an effect of a different viscosity of ASAR MP4, the setting kinetics, or – most likely – due to its fine microstructure. Comparing the ASAR MP4 SC and LC modes, both show considerable bulk cracking due to dehydration during the high vacuum-mode observation in the SEM. This behavior has no consequences for the clinical performance but rather reflects the material taking up and releasing water, indicating dimensional changes during the drying process in the SEM. It is certainly not correlated to the slightly inferior properties of the light-cured material (Fig 9d), but it shows a greater extent of cracking compared to the self-cured material (Fig 9c).

A further effect of light curing on material integrity might account for this behavior. In general, ASAR MP4 is a water-based system and thus susceptible to dehydration. In LC mode, the material was light cured directly after placement in the mold. As the susceptibility to dehydration was known, a thin Mylar strip was placed between the specimen surface and the glass plate in order to prevent dehydration. However, light curing in total was 200 s, a period in which the material continues to set chemically and also heats up upon photopolymerization. This procedure might have led to local, heat-induced dehydration or internal stress buildup, and may account for the early fractures of the LC material.

Based on the material properties measured for the novel self-adhesive product ASAR MP4, it can be discussed whether the material in self-cure as well as in light-cure mode may be considered for permanent clinical use. The FS, FFS, and  $K_{Ic}$  data of ASAR MP4 clearly reveal mechanical performance in the range of the successful permanent direct resin composites CeramX mono+ and Heliomolar. However, the mechanical performance represents only a limited view of the overall performance in a certain clinical indication. Hydrolytic degradation, expansion, and ion leaching must be considered for a broader picture, as this material is a hydrolytic system and its properties adjust over time. For example, a previous study showed decreasing mechanical performance for a resin composite material, while a GIC matures after placement over time, with the mechanical level reaching that of the resin composite after 6-month water storage.<sup>26</sup> A two-week storage period is already closer to clinical practice compared to ISO testing, but only long-term results might finally allow pre-clinical predictions.

## CONCLUSIONS

The overall mechanical performance of the novel self-adhesive restorative ASAR MP4 was ranked between that of GIC-based temporary and resin-based permanent filling materials. Processing the material in either self-cure or light-cure

mode led to superior performance over glass-ionomer-based cements.

From a practical standpoint, a self-adhesive condensable restorative material would be a beneficial development in filling technology. Not only the efficiency and reliability in dental treatment would increase by avoiding a laborious and technique-sensitive adhesive procedure, but also the accessibility for patients with lower socio-economic background is one central advantage for this type of material. As with many new technologies in restorative dentistry, this concept might present a compromise between mechanical performance and practical benefits that certainly requires further proof and clinical evidence, especially for use in permanent load-bearing class II indications.

## ACKNOWLEDGEMENTS

The materials tested in this study were kindly donated by Dentsply Sirona. The data shown resulted from research for Dentsply Sirona, and this study was financially supported by Dentsply Sirona. The authors disclose no other conflict of interest with Dentsply Sirona.

## REFERENCES

1. Alrahlah A. Diametral tensile strength, flexural strength, and surface microhardness of bioactive bulk fill restorative. *J Contemp Dent Pract* 2018; 19:13–19.
2. Bayne S, Petersen PE, Piper D, Schmalz G, Meyer D. The challenge for innovation in direct restorative materials. *Adv Dent Res* 2013;25:8–17.
3. Belli R, Petschelt A, Lohbauer U. Are linear elastic material properties relevant predictors of the cyclic fatigue resistance of dental resin composites? *Dent Mater* 2014;30:381–391.
4. Belli R, Wolf R, Petschelt A, Boccaccini A, Lohbauer U. The elastic-plastic nature of fracture in dental resin composites. *Dent Mater* 2015;31:e14–e5.
5. Braem M, Lambrechts P, Vanherle G. Clinical relevance of laboratory fatigue studies. *J Dent* 1994;22:97–102.
6. Braun AR, Frankenberger R, Kramer N. Clinical performance and margin analysis of ariston pHc versus Solitaire I as posterior restorations after 1 year. *Clin Oral Investig* 2001;5:139–147.
7. Danzer R, Lube T, Supancic P, Damani R. Fracture of Ceramics. *Adv Eng Mater* 2008;10:275–298.
8. Dixon WJ, Mood AM. A method for obtaining and analyzing sensitivity data. *J Am Stat Assoc* 1948;43:109–126.
9. Draughn RA. Compressive fatigue limits of composite restorative materials. *J Dent Res* 1979;58:1093–1096.
10. Drummond JL. Cyclic fatigue of composite restorative materials. *J Oral Rehabil* 1989;16:509–520.
11. Ferracane JL. Hygroscopic and hydrolytic effects in dental polymer networks. *Dent Mater* 2006;22:211–222.
12. Ferracane JL. Resin-based composite performance: Are there some things we can't predict? *Dent Mater* 2013;29:51–58.
13. Frankenberger R, Sindel J, Kramer N. Viscous glass-ionomer cements: a new alternative to amalgam in the primary dentition? *Quintessence Int* 1997;28:667–676.
14. Frankenberger R, Garcia-Godoy F, Lohbauer U, Petschelt A, Kramer N. Evaluation of resin composite materials. Part I: in vitro investigations. *Am J Dent* 2005;18:23–27.
15. Garcia-Godoy F, Frankenberger R, Lohbauer U, Feilzer AJ, Kramer N. Fatigue behavior of dental resin composites: Flexural fatigue in vitro versus 6 years in vivo. *J Biomed Mater Res B Appl BioMater* 2012;100B:903–910.
16. Heintze SD, Ilie N, Hickel R, Reis A, Loguercio A, Rousson V. Laboratory mechanical parameters of composite resins and their relation to fractures and wear in clinical trials – A systematic review. *Dent Mater* 2017;33: e101–e114.
17. Ilie N, Hilton TJ, Heintze SD, Hickel R, Watts DC, Silikas N, Stansbury JW, Cadenaro M, Ferracane JL. Academy of Dental Materials guidance – Resin composites: Part I – Mechanical properties. *Dent Mater* 2017;33: 880–894.

18. ISO. ISO 13586:2000. Plastics — Determination of fracture toughness (GIC and KIC) — Linear elastic fracture mechanics (LEFM) approach. Geneva: International Organization for Standardization, 2000.
19. Kirsten M, Matta RE, Belli R, Lohbauer U, Wichmann M, Petschelt A, Zorzin J. Hygroscopic expansion of self-adhesive resin cements and the integrity of all-ceramic crowns. *Dent Mater* 2018;34:1102–1111.
20. Klauer E, Belli R, Petschelt A, Lohbauer U. Mechanical and hydrolytic degradation of an Ormocer (R)-based Bis-GMA-free resin composite. *Clin Oral Investig* 2019;23:2113–2121.
21. Klee JE, Renn C, Elsner O. Development of novel polymer technology for a new class of restorative dental materials. *J Adhes Dent* 2020;22:xx-HERSTELLUNG! SEITEN EINGEBEN!.
22. Kramer N, Garcia-Godoy F, Reinelt C, Frankenberger R. Clinical performance of posterior compomer restorations over 4 years. *Am J Dent* 2006;19:61–66.
23. Lazaridou D, Belli R, Petschelt A, Lohbauer U. Are resin composites suitable replacements for amalgam? A study of two-body wear. *Clin Oral Investig* 2015;19:1485–1492.
24. Lazaridou D, Belli R, Kramer N, Petschelt A, Lohbauer U. Dental materials for primary dentition: are they suitable for occlusal restorations? A two-body wear study. *Eur Arch Paediatr Dent* 2015;16:165–172.
25. Lohbauer U, von der Horst T, Frankenberger R, Kramer N, Petschelt A. Flexural fatigue behavior of resin composite dental restoratives. *Dent Mater* 2003;19:435–440.
26. Lohbauer U, Frankenberger R, Kramer N, Petschelt A. Time-dependent strength and fatigue resistance of dental direct restorative materials. *J Mater Sci Mater Med* 2003;14:1047–1053.
27. Lohbauer U, Kramer N, Petschelt A, Frankenberger R. Correlation of in vitro fatigue data and in vivo clinical performance of a glassceramic material. *Dent Mater* 2008;24:39–44.
28. Lohbauer U. Dental glass ionomer cements as permanent filling materials? Properties, limitations and future trends. *Materials* 2010;3:76–96.
29. Lohbauer U, Belli R, Ferracane JL. Factors involved in mechanical fatigue degradation of dental resin composites. *J Dent Res* 2013;92:584–591.
30. Moraschini V, Fai CK, Alto RM, Dos Santos GO. Amalgam and resin composite longevity of posterior restorations: A systematic review and meta-analysis. *J Dent* 2015;43:1043–1050.
31. Munz D, Fett T. *Ceramics – mechanical properties, failure behaviour, materials selection*. Berlin: Springer, 2001.
32. Maas MS, Alania Y, Natale LC, Rodrigues MC, Watts DC, Braga RR. Trends in restorative composites research: what is in the future? *Braz Oral Res* 2017;31:e55.
33. Mount GJ. Glass-ionomer cements – past, present and future. *Oper Dent* 1994;19:82–90.
34. Opdam NJM, Bronkhorst EM, Loomans BAC, Huysmans MCDNJM. 12-year survival of composite vs. amalgam restorations. *J Dent Res* 2010;89:1063–1067.
35. Quinn JB, Quinn GD. A practical and systematic review of Weibull statistics for reporting strengths of dental materials. *Dent Mater* 2010;26:135–147.
36. Quinn JB, Quinn GD. Material properties and fractography of an indirect dental resin composite. *Dent Mater* 2010;26:589–599.
37. Quinn GD. On edge chipping testing and some personal perspectives on the state of the art of mechanical testing. *Dent Mater* 2015;31:26–36.
38. Sindel J, Frankenberger R, Kramer N, Petschelt A. Crack formation of all-ceramic crowns dependent on different core build-up and luting materials. *J Dent* 1999;27:175–181.
39. Regulation (EU) 2017/852 of the European Parliament and of the Council of 17 May 2017 on mercury. *Official J EU*. 2017;L137/1-21.
40. van Dijken JWV, Pallesen U, Benetti A. A randomized controlled evaluation of posterior resin restorations of an altered resin modified glass-ionomer cement with claimed bioactivity. *Dent Mater* 2019;35:335–343.
41. van Meerbeek B, Frankenberger R. Editorial: On our way towards self-adhesive restorative materials? *J Adhes Dent* 2019;21:295–296.
42. Wendler M, Belli R, Valladares D, Petschelt A, Lohbauer U. Chairside CAD/CAM materials. Part 3: Cyclic fatigue parameters and lifetime predictions. *Dent Mater* 2018;34:910–921.

**Clinical relevance:** Based on the mechanical performance investigated in this study, the novel self-adhesive restorative ASAR MP4 performed similar to the clinically successful resin composite materials Heliomolar and CeramX mono+. For clinical use, further aspects need to be considered and evidence should be based on clinical trials.